The Effects of Vertical Wind Shear on the Distribution of Convection in Tropical Cyclones

KRISTEN L. CORBOSIERO AND JOHN MOLINARI

Department of Earth and Atmospheric Sciences, University at Albany, State University of New York, Albany, New York

(Manuscript received 30 April 2001, in final form 6 March 2002)

ABSTRACT

The influence of vertical wind shear on the azimuthal distribution of cloud-to-ground lightning in tropical cyclones was examined using flash locations from the National Lightning Detection Network. The study covers 35 Atlantic basin tropical cyclones from 1985–99 while they were over land and within 400 km of the coast over water. A strong correlation was found between the azimuthal distribution of flashes and the direction of the vertical wind shear in the environment. When the magnitude of the vertical shear exceeded 5 m s^{-1}, more than 90% of flashes occurred downshear in both the storm core (defined as the inner 100 km) and the outer band region (r = 100–300 km). A slight preference for downshear left occurred in the storm core, and a strong preference for downshear right in the outer rainbands. The results were valid both over land and water, and for depression, storm, and hurricane stages. It is argued that in convectively active tropical cyclones, deep divergent circulations oppose the vertical wind shear and act to minimize the tilt. This allows the convection maximum to remain downshear rather than rotating with time.

The downshear left preference in the core is stronger for hurricanes than for weaker tropical cyclones. This suggests that the helical nature of updrafts in the core, which is most likely for the small orbital periods of hurricanes, plays a role in shifting the maximum lightning counterclockwise from updraft initiation downshear. The downshear right maximum outside the core resembles the stationary band complex of Willoughby et al. and the rain shield of Senn and Hiser. The existence and azimuthal position of this feature appears to be controlled by the magnitude and direction of the vertical wind shear.

1. Introduction

Vertical wind shear is known to have a negative correlation with intensity change in tropical cyclones at all stages of their life cycle (Gray 1968; DeMaria and Kaplan 1994; Hanley et al. 2001). Despite the importance of this parameter, the nature of its action remains uncertain. Many authors have noted the role of vertical wind shear in creating azimuthal asymmetries of convection in idealized numerical models of tropical cyclones (e.g., DeMaria 1996; Wang and Holland 1996; Frank and Ritchie 1999, 2001). Yet few observational studies have been done, and these typically cover only short periods in one or two storms, owing to the difficulty of observing tropical cyclones in nature.

The National Lightning Detection Network (NLDN) provides continuous coverage of cloud-to-ground lightning in space and time for all tropical cyclones over land and within roughly 400 km of the coastline. As a result, it is possible to determine the azimuthal lightning distribution as a function of the vertical wind shear for all tropical cyclones that have moved within range of the network since its origin in 1985. Molinari et al. (1994, 1999) and Samsury and Orville (1994) have shown that NLDN-determined lightning locations are sufficiently accurate to obtain insight into the structure and evolution of convection in tropical cyclones. The NLDN thus allows a considerable expansion of available case studies.

In the current paper, the effects of vertical wind shear on convective asymmetries in tropical cyclones, as measured by lightning frequency and distribution, will be evaluated. All named storms in the Atlantic basin that moved within range of the NLDN will be studied, both over ocean and over land, as long as they remained classified as tropical systems by the National Hurricane Center (NHC). The results will be compared to those predicted by theory and numerical modeling, and to previous observations using radar reflectivity, precipitation, and vertical motion. The data will also provide some insight into how tropical cyclones respond to vertical shear.

2. Review of vertical wind shear effects on tropical cyclones

a. Numerical studies

Reasor et al. (2000) have provided a review of vertical shear influences on vortices, including a formal quasi-

Corresponding author address: Kristen L. Corbosiero, Department of Earth and Atmospheric Sciences, SUNY Albany, 1400 Washington Ave., Albany, NY 12222.
E-mail: kristen@atmos.albany.edu

geostrophic framework for interpreting the various processes. Tropical cyclones represent strong vortices in relatively weak shear, in which vortex temperature gradients are much larger than those of the environment. The influence of vertical wind shear has been investigated using dry adiabatic dynamics by Raymond (1992), Jones (1995, 2000), DeMaria (1996), and Frank and Ritchie (1999). Four general influences on asymmetric vertical motion have been hypothesized (Jones 2000). First, because vertical shear in balanced flow is accompanied by horizontal temperature gradients, vortex flow along environmental isentropes will produce downshear upward motion [and upshear downward motion; Raymond (1992); Jones (1995)]. Second, as the vertical wind shear begins to tilt the vortex, a compensating secondary vertical circulation develops in an attempt to maintain balanced flow. This circulation, which also produces upward motion downshear and downward motion upshear (Raymond 1992; Jones 1995; DeMaria 1996), acts to move the vortex back toward a vertical orientation. In the adiabatic framework, this vertical circulation will create potential temperature anomalies in the vortex, with a cold anomaly downshear and a warm anomaly upshear of the storm center. The third influence on vortex asymmetries is vortex flow along these distorted vortex isentropes. This produces upward motion to the right of the vertical tilt vector, which is initially downshear (Raymond 1992). As time progressed, however, Jones (1995, 2000) found that vortex interactions in the vertical produced a rotation of the tilt vector away from downshear. Because upward motion is favored right of the tilt vector, the favored quadrant for upward motion also rotated in time. Finally, the fourth mechanism involves the relative flow (the environmental flow minus the motion of the vortex) along the vortex isentropes associated with the warm core. The pattern of vertical motion from the fourth effect depends on the vertical profiles of wind and potential vorticity in the vortex. Jones (2000) suggests that this last mechanism is secondary to the second and third mechanisms discussed above.

The previous mechanisms involve dry adiabatic dynamics only. In a ''full-physics'' numerical simulation of mature tropical cyclones, Frank and Ritchie (1999, 2001) argued that the temperature anomalies in the adiabatic simulations are no longer present in the saturated, precipitating storm core. They found the maximum upward motion lies persistently in the downshear left quadrant. A key result of Frank and Ritchie (2001) was that, even 48 h after the imposition of a 5 m s^{-1} shear, the vortex was virtually upright, but with a strongly asymmetric, quasi-steady vertical motion pattern, with maximum upward motion downshear left of the center.

Frank and Ritchie's (1999, 2001) integrations were on an f plane. Bender (1997) carried out similar integrations on a beta plane. The accompanying beta gyres produced flow across the vortex from the southeast that, like the vortex itself, weakened with height. A local shear from the northwest developed across the center as a result of the beta gyres, in the absence of any environmental shear. This shear reached a magnitude of nearly 5 m s^{-1} between 850 and 200 hPa. It produced, as would be expected, upward motion downshear (southeast of the center) in a quiescent environment. The evidence suggests that, with regard to convective asymmetries in the tropical cyclone core, the beta effect can be treated simply as an additional vertical shear effect.

None of the idealized numerical modeling studies previously discussed produced significant outer rainbands. Using the definition of Molinari et al. (1994, 1999), these are bands that initiate (or possibly first become electrified) outside the central dense overcast of the tropical cyclone. They reach their maximum intensity, measured by average lightning flash density over several storms, about 250 km from the storm center (Molinari et al. 1999). More lightning occurs in outer rainbands than in any other part of tropical cyclones (Lyons and Keen 1994; Molinari et al. 1994; Samsury and Orville 1994; Cecil and Zipser 1999). Lightning activity will thus be useful for examining asymmetries in such bands that cannot be seen using current numerical modeling studies.

b. Observational studies

As noted earlier, only a few observational studies have examined the influence of vertical wind shear on convective asymmetries in tropical cyclones. In the core of strong tropical cyclones, the updrafts rise helically (Franklin et al. 1993). The latter relates to (i) the small convective instability (Bogner et al. 2000) and thus relatively small vertical motions (Black et al. 1996) in the core, and (ii) the large tangential velocity and thus small orbital period in the core of strong storms. The helical updraft arises because the time required for a parcel to rise from the surface to the tropopause and the orbital time period are of the same magnitude. As a result, an azimuthal separation develops between updraft initiation, maximum updraft velocity, and maximum precipitation. In the presence of moderate or strong vertical shear, the maximum eyewall reflectivity can be as much as 180° of azimuth counterclockwise from the azimuth of updraft initiation, literally upshear (Franklin et al. 1993). Frank and Ritchie (2001) simulated this structure; their maximum rainfall extended from 90° left of the shear vector around to upshear in the eyewall, even while maximum upward motion remained about 45° left of the shear vector.

Observational studies show a relatively consistent influence of vertical wind shear in the storm core (Franklin et al. 1993; Gamache et al. 1997; Reasor et al. 2000). In general, updrafts initiate downshear, maximum vertical motion in the core is downshear left, and maximum precipitation is further displaced counterclockwise. This structure was present for vertical wind shear magnitudes

of 7–15 m s^{-1}. When vertical shear was 3 m s^{-1}, reflectivity patterns were much closer to axisymmetric (Gamache et al. 1997; Reasor et al. 2000). None of these papers considered convective asymmetries outside the core region.

Willoughby et al. (1984) produced a schematic diagram of radar reflectivity in tropical cyclones that included convective structure outside the core. In Willoughby et al.'s diagram, high reflectivity in the eyewall extended in a counterclockwise direction from directly downshear to directly upshear, similar to the structure described earlier. Outside the tropical cyclone core they described a ''stationary band complex'' (SBC) that occurred downshear at radii of approximately 80–120 km. The SBC contained a dominant band (the ''principal band'') plus a number of typically nonconvective secondary bands closer to the center. The schematic of Willoughby et al. (1984) does not extend beyond the 150-km radius because reconnaissance aircraft do not routinely sample larger radii. The SBC resembles the ''rain shield'' described in tropical cyclones by Senn and Hiser (1959) using radar data. The rain shield was a quasi-stationary region (with respect to the moving center) they described as a ''graveyard for rainbands'' that had earlier propagated outward from inner radii.

The current study will examine the problem using cloud-to-ground lightning. The results will provide a measure of asymmetries in active convection over a large number of storms of varying intensity, over water and over land, for three ranges of vertical wind shear magnitude.

3. Data

a. NLDN

Lightning data were obtained from archived observations of the NLDN, which was originally developed at the University at Albany, and is currently operated and maintained by Global Atmospherics, Inc. (GAI) of Tucson, Arizona. Full descriptions of the operation and equipment of the NLDN can be found in Krider et al. (1976), Orville et al. (1987), Orville (1991) and Cummins et al. (1992, 1998).

As with all remotely sensed data, caution must be used when interpreting the results. As long as the storms are within 400 km of at least one sensor, the decrease in detection efficiency with increasing distance from the NLDN seems not to be as important as the physical and dynamical processes within the hurricane itself in determining the spatial distribution of flashes (Molinari et al. 1999). Over the continental United States detection efficiency was noted to be in the range of 50%–80% from 1985–94 (Orville et al. 1987; Cummins et al. 1992; Orville 1994). According to Cummins et al. (1992), 50% of flashes detected inside the original network are accurate within 8 km, except for the region between the south tip of Florida and Cuba where errors associated with the geometry of the sensors affect the location of flashes. This number is in agreement with Orville (1994) who cites a network accuracy between 4–8 km in the years 1989–91.

After the major upgrade and reconfiguration of the network in 1994, Cummins et al. (1998) found that, according to their idealized model, the upgraded network should have a detection efficiency of 80%–90% and a mean accuracy of 0.5–1.0 km over much of the continental United States for flashes over 5 kA (their Fig. 7). The exception is again the area south of Key West, Florida, where the projected detection drops to 40% and the location errors may be as great as 8–10 km. Idone et al. (1998a,b) carried out tests in Albany, New York, during the summers of 1994–96 using video cameras to record lightning flashes. They found ground flash detection efficiencies of 67% before the upgrade in 1994, and 72% in 1996 after the completion of the upgrade. Location accuracy was 2.61 km in 1994 and 0.435 km in 1995, representing a substantial improvement in upstate New York from the previous configuration of the network.

Based on the results of these earlier studies, it is expected that the updated network will sense a larger fraction of existing flashes, with greater location accuracy, in storms occurring during and after 1994, versus the 1985–93 period. In this study, the spatial distribution of flashes is of primary interest. This distribution should not be influenced by changes in detection efficiency as long as a sufficient sample of flashes is present (see section 4b). As a result, no further delineation of the old and new NLDN configurations will be made.

b. ECMWF analyses

Vertical wind shear calculations were made using gridded analyses from the European Centre for Medium-Range Weather Forecasts (ECMWF). The grids contain 12 (13 after 1992) vertical pressure levels and 1.125° latitude–longitude horizontal resolution. The grids are interpolated bilinearly in the horizontal (Molinari and Vollaro 1989) to yield cylindrical grids, centered on the NHC best track storm position, with $dr = 100$ km and $d\lambda = 5°$.

Following Hanley et al. (2001), a cylindrical area-weighted average of the Cartesian components of the mean wind were computed over a radius of 500 km from the storm center. This averaging removes a symmetric vortex so that the resulting winds are a measure of the cross-storm flow at each level. The vertical wind shear is then calculated from these mean winds between 850 and 200 hPa every 12 h.

Because the cylindrical grids are centered on the observed positions from NHC, the difference in center position between the NHC best track dataset and the ECMWF analyses is a potentially important issue. Molinari et al. (1992) found the average position error of the gridded analyses for Hurricane Elena (1985) was

about 120 km. Because of this discrepancy between the centers, the area-average calculation for mean wind components was done over 500 km even though this study focuses on lightning over only the 300 km surrounding the storm. The larger radius was chosen in order to maximize the overlap between the areas surrounding the ECMWF and NHC centers.

Molinari and Vollaro (1990) objectively analyzed a special set of satellite-derived cloud drift winds at 200 hPa for Hurricane Elena (1985). The vector difference in that study between the mean objectively analyzed wind averaged over a 500-km radius from the storm center and the mean wind over the same region from the ECMWF gridded analyses has since been calculated (D. Vollaro 2001, personal communication). The median value of this vector difference over 12 analysis times was found to be 1.4 m s^{-1}. This provides a measure of uncertainty in the mean wind from the ECWMF analyses at the 200-hPa level for storms near the United States coast. Because the vector errors could either add or cancel between 850 and 200 hPa, it is estimated that median errors in calculated 850–200-hPa vertical wind shear in this paper will be 1–2 m s^{-1}.

The vertical wind shear categories that will be used in this study are 0–5, 5–10 and >10 m s^{-1}. As a result, although errors in the estimated shear will shift some time periods into an adjacent category, we do not anticipate a significant bias will be introduced by the errors in the estimates of vertical shear. In addition, Molinari et al. (1995) noted the accuracy of ECMWF analyses of storms relatively close to the rawinsonde network over the United States mainland. Because this study is restricted to storm centers within 400 km of the coastline, the vertical wind shear estimates from the ECMWF analyses are likely to be sufficiently accurate.

It was noted earlier that the beta effect can be considered simply an additional influence of vertical shear, in that it induces a northwesterly vertical wind shear of up to 5 m s^{-1} added to the environmental shear. In the ECMWF analyses, a beta effect must be present, because the ECMWF model contains a simulated vortex in the presence of a variable Coriolis parameter. The simulated tropical cyclone vortex in the global model will most likely be larger and weaker than that in nature. An unrealistically large vortex would have stronger beta gyres, and a weaker vortex would have weaker beta gyres, compared to their actual structure in nature. It is thus likely that errors partially offset in the simulated beta gyres, and the vertical wind shear associated with beta gyres is likely represented to some degree by the gridded analyses. As a result, no adjustments of the calculated shear were made to account for the beta effect.

c. NHC Best Track

Tropical cyclone latitude, longitude, and intensity were obtained at 6-h intervals from the NHC best track dataset. Between the available center position times, the data were linearly interpolated to estimate the hourly center positions of the storms. Table 1 lists the 35 Atlantic basin tropical cyclones examined in this study and the times their centers were in range of the NLDN (i.e., within 400 km of at least one magnetic field sensor). For each of the hours listed, flashes were totaled and plotted with respect to the interpolated hourly center position. Because the ECMWF analyses were taken twice daily, the hourly periods were grouped together into two 12-h periods each day centered on the analysis times (i.e., 0600–1800 UTC and 1800–0600 UTC). Furthermore, if a storm made landfall within a given 12-h period, the period was subdivided into separate pre- and postlandfall periods. This grouping of the data yields a total of 303 individual (mostly 12-h) time periods, the breakdown of which, by storm, is shown in Table 1. The results of this study will not be grouped by storm. Rather, each of the 303 time periods will be treated as an individual data point with its own unique vertical wind shear vector and lightning distribution.

4. Methodology

a. Choice of radial ranges

A common radial distribution of lightning was first observed by Molinari et al. (1994, 1999) in Atlantic basin hurricanes: a weak eyewall maximum 20–60 km from the center, a clear minimum in flash density somewhere between the 60- and 140-km radii, and a strong maximum in the outer rainbands, 200 to 300 km from the storm center. Summed over nine hurricanes, the flash minimum occurred in the radial bin between 100 and 120 km (Molinari et al. 1999, their Fig. 4). Thus for hurricane-strength disturbances, a radius of 100 km represents a good choice for a dividing line between inner and outer regions for this study. Molinari et al. (1994) proposed that formation of an eyewall creates the distribution described above, because debris from the eyewall creates a mesoscale anvil region of falling hydrometeors outside the eyewall that suppresses deep convection. In tropical cyclones of less than hurricane strength, which are unlikely to have well-developed eyewalls, the radii of flash maxima and minima are more variable (Molinari et al. 1999, their Fig. 6). In principle an optimum radius of division between inner and outer regions could be defined storm by storm, but because the data in this study will be divided into individual 12-h periods, this procedure is potentially arbitrary and misleading. The 100-km radius will be chosen as the dividing line for all time periods. The region inside 100 km will be referred to as the inner core, and the 100–300-km radii will be referred to as the outer band region.

b. Minimum flash criteria

On average per 12-h time period over all storms, 162 flashes occurred within the inner core and 1475 flashes

TABLE 1. List of storms and the hours they were within range of the NLDN. ''Individual time periods'' refers to the number of 12-h periods into which the lightning data for each storm was divided, to correspond to the twice-daily vertical shear values from ECMWF gridded analyses. The last two columns are the number of time periods that met the minimum flash criterion for the inner core and outer rainband regions, respectively.

Storm	Begin/end time	H	Individual time periods	Inner core >100 flashes	Outer rainband >400 flashes
Bob 1985	1800 UTC 21 Jul 1800 UTC 25 Jul	96	10	6	8
Danny 1985	0600 UTC 17 Aug 2300 UTC 18 Aug	41	4	1	2
UTS 1987	0000 UTC 11 Aug 0500 UTC 17 Aug	149	13	9	11
Chris 1988	0600 UTC 27 Aug 0500 UTC 29 Aug	47	5	1	2
Florence 1988	1800 UTC 9 Sep 0600 UTC 11 Sep	36	4	0	0
Allison 1989	0100 UTC 25 Jun 2300 UTC 27 Jun	70	8	4	6
Chantal 1989	0000 UTC 1 Aug 2300 UTC 2 Aug	47	6	3	3
Jerry 1989	1200 UTC 15 Oct 1700 UTC 16 Oct	29	4	3	0
Marco 1990	1300 UTC 9 Oct 1100 UTC 12 Oct	70	8	6	6
Bob 1991	0000 UTC 17 Aug 1700 UTC 20 Aug	89	8	0	4
Andrew 1992	0000 UTC 24 Aug 0600 UTC 28 Aug	102	12	0	8
Danielle 1992	0000 UTC 25 Sep 1100 UTC 26 Sep	35	5	2	2
Alberto 1994	1200 UTC 2 Jul 1200 UTC 7 Jul	120	12	8	9
Beryl 1994	1200 UTC 14 Aug 0000 UTC 19 Aug	108	11	1	7
Gordon 1994	0800 UTC 14 Nov 0600 UTC 19 Nov 0900 UTC 20 Nov 1800 UTC 21 Nov	151	16	0	2
Allison 1995	0600 UTC 5 Jun 0600 UTC 6 Jun	24	2	2	0
Dean 1995	1300 UTC 29 Jul 1200 UTC 1 Aug	71	8	7	7
Erin 1995	1300 UTC 1 Aug 1200 UTC 6 Aug	119	14	0	6
Jerry 1995	1800 UTC 22 Aug 0000 UTC 28 Aug	126	12	4	10
Opal 1995	0700 UTC 4 Oct 1800 UTC 5 Oct	35	3	1	1
Arthur 1996	1800 UTC 17 Jun 1800 UTC 20 Jun	72	7	4	4
Bertha 1996	1800 UTC 10 Jul 0600 UTC 14 Jul	84	8	2	2
Fran 1996	0000 UTC 5 Sep 0000 UTC 9 Sep	96	9	1	0
Josephine 1996	1200 UTC 6 Oct 0600 UTC 8 Oct	42	4	2	1
Danny 1997	1800 UTC 16 Jul 1800 UTC 24 Jul	192	17	13	16
Charley 1998	0600 UTC 21 Aug 1800 UTC 23 Aug	60	6	3	2
Earl 1998	1200 UTC 1 Sep 1800 UTC 3 Sep	54	5	2	5
Frances 1998	1800 UTC 8 Sep 1800 UTC 13 Sep	120	10	0	1
Georges 1998	1800 UTC 24 Sep 0600 UTC 1 Oct	156	14	1	5
Hermine 1998	1200 UTC 17 Sep 1800 UTC 20 Sep	78	7	5	3

TABLE 1. (*Continued*)

Storm	Begin/end time	H	Individual time periods	Inner core >100 flashes	Outer rainband >400 flashes
Bret 1999	1800 UTC 8 Aug 0000 UTC 25 Aug	78	8	2	8
Dennis 1999	1800 UTC 28 Aug 1800 UTC 7 Sep	120	21	4	5
Floyd 1999	1800 UTC 13 Sep 1200 UTC 17 Sep	90	8	0	0
Harvey 1999	0600 UTC 20 Sep 0000 UTC 22 Sep	42	5	4	5
Irene 1999	0600 UTC 15 Oct 0000 UTC 19 Oct	90	9	5	3

within the outer band region. When these values are normalized by area, the two regions have almost equal flash densities of 52 and 58 flashes per $(100\ km)^2$ per 12 h, respectively. A huge range of flash counts occurred over 12-h periods, from zero to several thousand. Because the azimuthal distribution of flashes is not meaningful for low-flash counts, a lower limit flash criterion was formulated to restrict the number of cases examined. Minimum counts of 50 and 400 flashes per time period were chosen for the inner core and outer band regions, respectively. When the area of each region is taken into account, the flash density criteria are equal for the two regions, at approximately 16 flashes per $(100\ km)^2$ per 12 h. This value was chosen to maximize the number of time periods while excluding those periods in which flashes were too few for a meaningful estimate of the quadrant of maximum lightning activity.

With these flash count criteria applied, 106 inner core and 154 outer rainband region time periods remained of the original 303. The number of times that met the flash criteria, by storm, are listed in the last two columns of Table 1.

The elimination of 12-h periods with low flash counts preferentially removes storms with certain characteristics. Specifically, the percentage of hurricane-strength disturbances was reduced in both the inner core and outer band regions, and the percentage of high-shear ($>10\ m\ s^{-1}$) time periods was reduced in the outer rainband region. Further details of these results can be found in the appendix.

c. Quantification of the azimuthal distribution

Compared to the radial distribution of lightning, the azimuthal distribution of flashes has received far less attention. Samsury and Orville (1994) noted in their study of Hurricanes Hugo (1989) and Jerry (1989) that the majority of flashes in both storms occurred to the east of the centers. A similar pattern was found by Molinari et al. (1994) in Hurricane Andrew, where 40% of the recorded flashes out to 300 km occurred in the northeast quadrant of the storm. Molinari et al. (1999) plotted all flashes occurring within 300 km of the centers of nine Atlantic tropical cyclones during the hurricane stage only. The majority of flashes in the outer rainbands occurred to the south and southeast of the storm centers with a minimum in flash count to the northwest of the center.

Table 2 contains the flash counts per storm-centered quadrant for the 106 inner core and 154 outer rainband region time periods meeting the minimum flash criterion. In the inner core, three-quarters of the flashes occurred in the eastern half of the storms, with a maximum in the southeast quadrant, consistent with previous studies. The majority of outer rainband flashes (68%) occurred to the south of the center, with a maximum in the southeast quadrant and a minimum in the northwest quadrant, comparable to the results of Molinari et al. (1999).

The straight flash counts per quadrant are skewed by storms that contained large amounts of lightning. For example, 21% of the 54 000 inner core flashes noted in Table 2 were from 11 Tropical Storm/Hurricane Danny (1997) time periods (Table 1), and another 12% from six Hurricane Bob (1985) time periods. Thus 33% of the flashes were from only 16% of the time periods.

In order to avoid having a few extreme events dominate the distribution, the preferred quadrant for lightning in each 12-h period will be defined simply by the quadrant with the most flashes. The number of times

TABLE 2. Two ways of quantifying the azimuthal distribution of lightning: 1) The total number of flashes that occurred in each quadrant, and 2) the number of 12-h periods the flash count was highest in each quadrant.

Region	Method	Northwest	Northeast	Southeast	Southwest
Inner core	Flashes	8196	13 493	27 213	4987
	Highest flash count	24	28	42	12
Outer band	Flashes	41 422	77 024	128 131	117 955
	Highest flash count	16	45	63	30

each quadrant was the one with the highest flash count over all time periods appears in Table 2. This latter measure will be used to compare the lightning distribution across multiple time periods.

d. Rotation of flash locations

In order to evaluate the effect of the vertical wind shear on the distribution of lightning, the flashes in each time period were rotated around the storm center so that the shear vector for the period was pointing due north. The quadrant with the highest number of flashes after this rotation was then determined. Data will be examined in this shear-rotated coordinate system in the remainder of this paper.

5. Vertical wind shear influences

a. Inner core region

Figures 1a–c show all ground flashes occurring within the inner core region for the weak-, medium-, and strong-shear time periods, respectively, rotated so that the shear vector in each case is pointing due north. The weak-shear plot has the most symmetric distribution of the three, but still has the majority (69%) of flashes downshear. The medium-shear distribution contains the largest number of flashes and also shows a clear downshear signal (90% of flashes). Almost all of the flashes during strong-shear time periods occur in the downshear quadrants (93%) with a slight downshear left preference. Thus, as the strength of the vertical shear increases so does the strength of the downshear relationship.

Figure 2 provides similar information to Fig. 1, but in terms of the number of time periods in the inner core for which the flash count was highest in each of the shear-rotated quadrants. The upper two squares in each box represent the downshear quadrants.

The lower-right box of the figure gives the sum over all magnitudes of shear. It shows that 86% (91 of 106) of time periods appear in the downshear quadrants of the storms in the inner core. The strength of this relationship increases with the strength of the shear: highest flash counts appear downshear in 65% of time periods for weak shear, 91% for medium shear, and 93% for strong shear. Weak- and medium-shear time periods exhibit no downshear left or right preference, while the strong-shear time periods show a definite downshear left signal that carries over to the overall distribution for the inner 100 km and produces a downshear left preference for core lightning strikes. These numbers are similar to the absolute flash count percentages given previously, except that Fig. 2 shows a different quadrant of maximum activity than Fig. 1 for medium shear. As noted earlier, this reflects the artificially large influence of a few storms with very high flash counts. The quadrant plots of Fig. 2 give a more representative measure of the behavior over a large number of tropical cyclones.

It is apparent from Fig. 2 that vertical wind shear has an enormous influence on the organization of convection containing cloud-to-ground lightning in the inner core of tropical cyclones. For values of shear greater than 5 m s^{-1}, the direction of the shear appears to be the major factor in the observed convective asymmetries in the tropical cyclone core.

b. Outer rainband region

Figure 3 shows all of the shear-rotated flashes occurring in the outer rainbands for the 45 time periods with strong vertical shear. Eighty-five percent of the 80 844 flashes occurred downshear of the center. A strong preference for the downshear right quadrant was seen, with 63% of flashes in this quadrant. This maximum in flash count is located approximately 90° clockwise from the downshear left maximum in the inner core seen in Fig. 1c.

Figure 4 shows the same quadrant plots as Fig. 2, but for the outer rainband region. A strong correlation between the direction of the vertical wind shear vector and the azimuthal distribution of lightning is evident, with a greater percentage of time periods having their highest flash frequency downshear as the magnitude of the shear increases. Sixty-one of the 70 (87%) medium-shear and 39 of 45 (87%) strong-shear time periods have maximum lightning in the downshear quadrants. Weak-shear time periods have a neither a downshear left nor right preference, while medium- and strong-shear time periods show a strong downshear right signal. The quadrant plot of the sum over all strengths of shear (lower-right box of Fig. 4) shows that 84% of the quadrants having the highest flash frequency lie downshear and 54% downshear right.

Overall, as the strength of the shear increases, a larger percentage of time periods in the outer rainband region have their highest flash counts downshear and, moreover, downshear right. Thus it appears that the azimuthal distribution of cloud-to-ground flashes in the outer rainbands, like that of the inner core, is dictated to a large degree by the direction and magnitude of the vertical wind shear.

c. Influences of storm intensity and underlying surface

In the above distributions, storm time periods were broken down into categories based upon the strength of the vertical wind shear, with no consideration given to storm intensity or the surface over which the storm was moving during the time period. These two effects will be addressed in this section. To facilitate comparison, the tables in this section will show the *percentage* of 12-h periods that each quadrant contained the flash maximum, rather than the number of such periods as previously shown. Table 3 shows the percentage of time periods the flash count was highest per shear-rotated

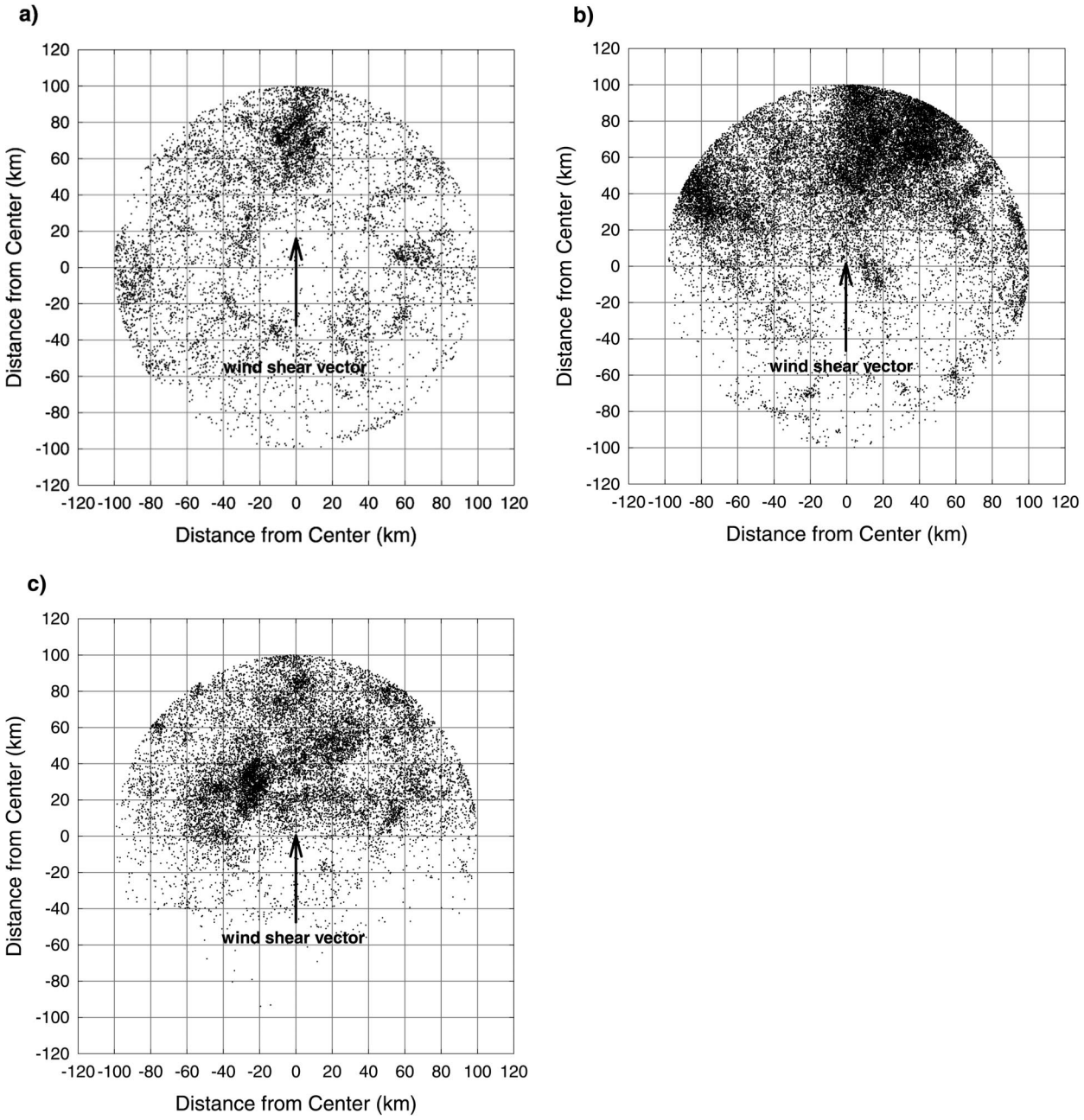

FIG. 1. Locations of all flashes occurring within 100 km of the storm centers in the (a) 23 weak-shear, (b) 43 medium-shear, and (c) 40 strong-shear time periods that met the minimum flash criterion. The flashes have been rotated around the center so that the vertical wind shear vector for each time period is pointing due north.

quadrant for the inner core and outer rainband regions, broken into the three standard intensity categories. In both regions, the strongest downshear signal is seen in the tropical storm time periods (~90% downshear), followed by the tropical depression and the hurricane time periods (~80% downshear). In the core, the downshear left signal discussed in the previous section is seen to increase with increasing average intensity. In the outer band region, the strong downshear right signal noted above decreases slightly with increasing storm intensity.

Table 4 shows the percentage of times the flash count was highest per shear-rotated quadrant for time periods when the storm center was over land versus over water. The most striking aspect of Table 4 is the large degree of agreement between the two underlying surfaces. There is no significant difference between land and water in the outer rainband region, while the left of shear signal is slightly more prominent in the inner core over land. Overall, the results of this section show that the strong influence of vertical wind shear on the azimuthal

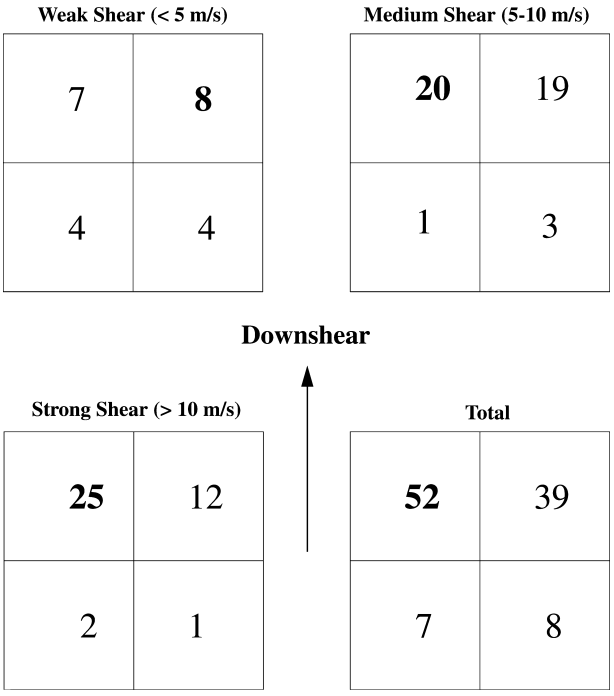

FIG. 2. Quadrant plots showing the number of times the flash count was highest per shear-rotated quadrant for weak-, medium-, and strong-shear time periods. The center of each box represents the storm center, and flash locations were rotated such that the vertical wind shear vector points due north. The upper two quadrants of each box represent the downshear direction.

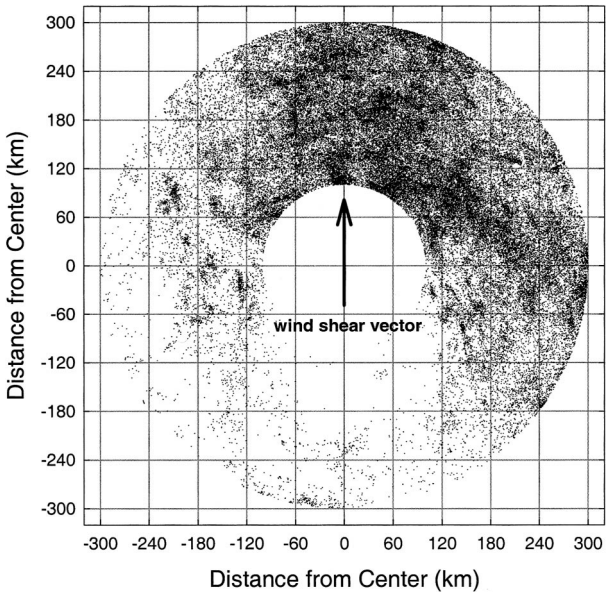

FIG. 3. Locations of all flashes occurring in the outer band region of the 45 individual time periods with strong shear that met the minimum flash criterion. The flashes have been rotated around the center so that the vertical wind shear vector for each individual time period is pointing due north.

distribution of active convection holds regardless of storm intensity or underlying surface.

d. Composite structure of two tropical cyclones

In this section, composite lightning plots of two storms, Hurricane Bertha (1996) and Tropical Storm/Depression Alberto (1994), will be presented. These storms have been chosen because they contain all of the features discussed in the above sections. It is important to note that all storms do not behave in this manner. For example, many individual time periods contain only an outer rainband maximum in lightning, with very few core flashes, while some time periods contain explosive core outbreaks in lightning and relatively inactive outer rainbands.

Figure 5a shows the total cloud-to-ground lightning flashes within 300 km of the center of Hurricane Bertha (1996) from 0600 UTC 11 July to 0600 UTC 14 July. The flashes have been rotated around the center to align the vertical wind shear vector with due north for each 12-h period. Bertha (1996) was a category 1 or 2 hurricane throughout the time periods shown in Fig. 5a as it moved towards the north embedded in an environment of strong westerly vertical shear. Bertha made landfall on the North Carolina coastline at 2000 UTC 12 July, so that of the seven time periods in Fig. 5a, five are over water. Many features of the typical radial distribution of lightning in hurricanes presented by Molinari et al. (1999) are seen. An eyewall peak in flashes is observed between 30 and 60 km from the center. This

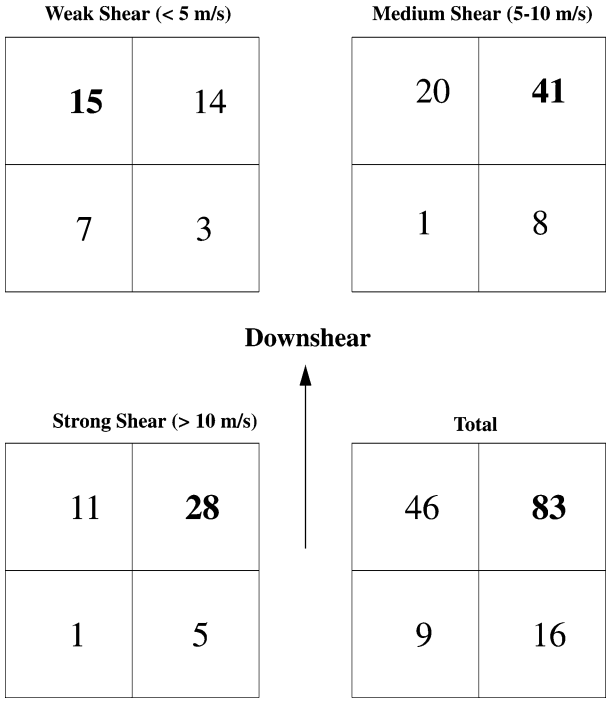

FIG. 4. Same as in Fig. 2, except for the outer rainband time periods meeting the minimum flash criterion.

TABLE 3. Percent of 12-h time periods that the flash count was highest per shear-rotated quadrant, broken down as a function of storm intensity.

Region	Category	Downshear left	Downshear right	Upshear right	Upshear left
Inner core	Tropical depression	47	35	7	11
	Tropical storm	49	43	6	2
	Hurricane	56	25	0	19
Outer rainband	Tropical depression	23	57	11	9
	Tropical storm	39	54	5	2
	Hurricane	29	47	18	6

outbreak exists directly downshear of the center with no left or right preference. A distinct minimum in flash density is noted 100–180 km from the center in the weakly electrified inner band region described by Molinari et al. (1994, 1999). Outward of 180 km, bands of flashes curve around the center from directly downshear of the storm to the right of shear.

Figure 5b shows the vertical wind shear–rotated flashes occurring within 300 km of the center of Tropical Storm/Depression Alberto (1994) from 0600 UTC 3 July to 0600 UTC 6 July. The six time periods plotted are all after Alberto made landfall on the Florida panhandle. During this time the storm weakened and drifted slowly toward the northeast in an environment of moderate north-northwesterly wind shear. Several differences between the distributions in Figs. 5a and 5b can be seen. The most obvious is the larger number of flashes (15 989 vs 2996) in Alberto (1994). This difference is consistent with the greater electrification expected of weaker tropical cyclones (Molinari et al. 1999). It is also consistent with the results presented in the appendix, in that the magnitude of the shear in Hurricane Bertha (1996) was almost twice that of Tropical Storm Alberto (1994); larger shear tended to be associated with fewer flashes in the outer rainbands.

The distinct radial distribution of flashes seen in Hurricane Bertha (1996) (eyewall maximum, inner rainband minimum, outer rainband maximum) is not observed in Tropical Storm/Depression Alberto (1994). Instead, the latter has no clear-cut minimum between the storm core and outer bands. Molinari et al. (1999) argued that tropical storm or weaker disturbances lack a well-defined eyewall, and thus lack the convective suppression associated with the melting and evaporation of hydrometeors ejected from the eyewall. The inner peak of flashes in Alberto (1994) is more diffuse and located farther from the center, 60–100 km, than in Bertha (1996). This is consistent with the results of Heller (1999), who found weaker hurricanes and tropical storms had inner peaks that were located at larger radii and covered a larger area than strong hurricanes.

TABLE 4. Percent of 12-h time periods that the flash count was highest per shear-rotated quadrant, for inner core and outer rainband regions, at times the tropical cyclone centers were over land vs over water.

Region	Downshear left	Downshear right	Upshear left	Upshear right
Land inner core	54	32	6	8
Water inner core	45	41	9	5
Land outer rainband	30	53	11	6
Water outer rainband	33	52	10	5

The point to note from Figs. 5a and 5b is the strikingly similar azimuthal distribution of convection with respect to vertical wind shear. The large majority of flashes within 100 km of the center appear downshear, while flashes in outer rainbands are most frequent downshear right. The inner flash maxima tend to be quasi-circular, while the flashes in the outer region tend to be elongated into banded structures. This distinct distribution is seen for two storms with different intensities, different magnitudes of shear, and different underlying surfaces.

6. Discussion

The clearest signature in the lightning distribution is the strong preference for maxima in the downshear quadrants in both the inner core ($r < 100$ km) and outer rainband region ($r = 100$–300 km) of tropical cyclones. This basic result held equally well over land and over water, and for tropical cyclones of all intensities. The simplest explanation for this behavior comes from the work of Frank and Ritchie (2001). They showed that for vertical shear of up to 10 m s^{-1} over the depth of the troposphere, a simulated hurricane-strength vortex remained upright, but with strong asymmetric vertical circulations, for 24–30 h after the shear was imposed. Essentially a balance occurred between the tendency of the vertical shear to tilt the vortex and the action of deep, convectively driven circulations to force it back toward a vertical orientation. To the extent that such a balance occurs, the favored region for upward motion would remain downshear, as was observed in this study.

Frank and Ritchie (2001) also found that maximum vertical motion occurred in the downshear left quadrant in their moist simulations. They argued that updrafts initiate downshear and rise helically. The helical updraft develops because orbital periods are so small in the core of hurricanes. Based upon this reasoning, the maximum lightning frequency should be shifted counterclockwise from downshear. This is supported by the results of this paper shown in Table 3: the downshear left maximum

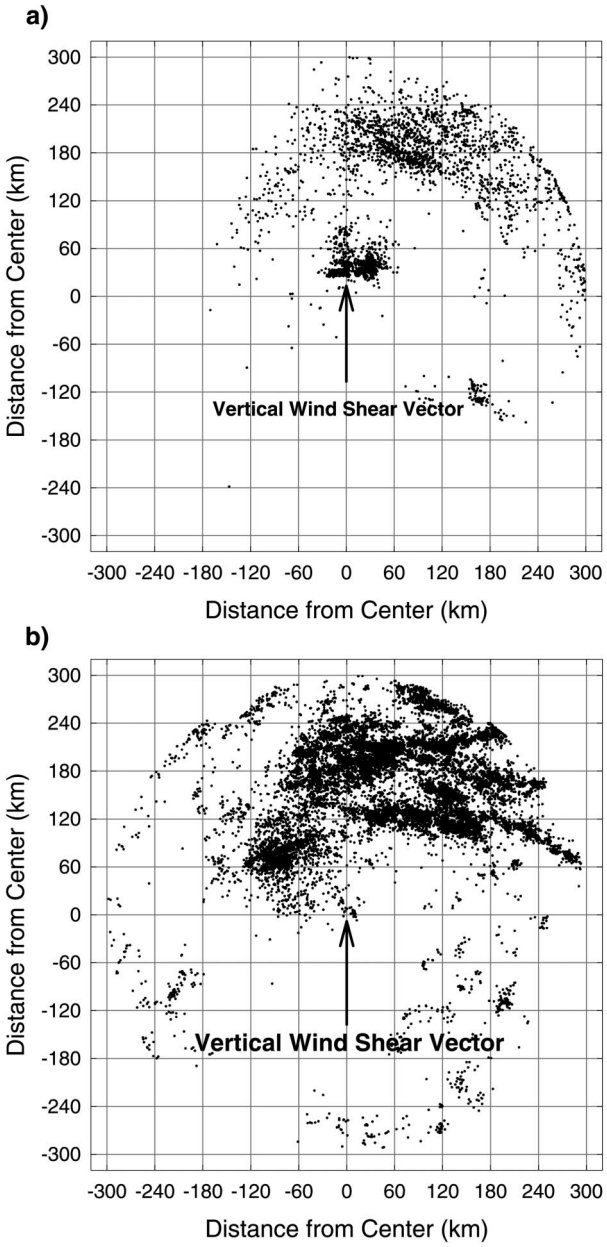

FIG. 5. Total lightning flashes within 300 km of the centers of (a) Hurricane/Tropical Storm Bertha (1996) from 0600 UTC 11 Jul to 0600 UTC 14 Jul and (b) Tropical Storm/Depression Alberto (1994) from 0600 UTC 3 Jul to 06 UTC 6 Jul. The flashes have been rotated around the storm center so that the vertical wind shear vector for each individual time period is pointing due north.

and upshear right minimum in lightning were less pronounced in depressions and storms than in hurricanes. The weaker storms have greater orbital periods, because their maximum winds are weaker and generally at larger radii. The result is a smaller cyclonic shift of the updraft with height, and less of a left-of-downshear signature, as shown in Table 3.

Two potential difficulties occur with the reasoning of Frank and Ritchie (2001). First, their simulations used a 5-km grid spacing. With such resolution it is difficult to meaningfully resolve, for instance, a 5-km tilt of the storm center from the lower to the upper troposphere. Yet a 5-km tilt in a 15-km-deep troposphere is significant. The reasoning above also does not account for the clockwise rotation of the preferred region for convection to downshear right outside the 100-km radius.

An alternative explanation comes from the adiabatic simulations of Jones (1995, 2000). In her simulations, the direction of vortex tilt rotated cyclonically away from the downshear direction due to vortex interactions in the vertical. When potential vorticity was used to define the vortex centers in her simulations, the separation from near the surface to the 6-km level exceeded 50 km and the tilt vector had turned almost 90° from downshear after 12 h. The cold anomaly in the downtilt direction must also shift 90° in a balanced vortex. Using adiabatic reasoning, vortex flow on the resultant distorted vortex isentropes would produce upward motion downshear, right of the tilt vector (Jones 2000; Reasor et al. 2000). In Jones's adiabatic simulations, however, the tilt axis continued to rotate to 180° from the vertical shear direction after 24 h. Given the persistent downshear convection found in this study, 180° rotation of the tilt axis seems unlikely in nature.

Few observations of tropical cyclone tilt exist. Reasor et al. (2000) found a downshear tilt of 3 km from near the surface to the midtroposphere, and no more than 8 km from the surface to the top of the troposphere. These tilts occurred in Hurricane Olivia, which contained strong convection and was experiencing vertical wind shear in a range of 3 to 15 m s^{-1} over 10 km. Additional information on vortex tilt must come from high-resolution numerically simulated tropical cyclones. Recently, R. Rogers (2001, personal communication) simulated the behavior of Hurricane Bonnie (1998) using 1.67-km grid spacing. When vertical wind shear exceeded 20 m s^{-1}, tilt averaged 12–13 km between 900 and 400 hPa. When the shear dropped to order 7 m s^{-1}, comparable to the mean shear in the storms in this study, tilt dropped to about 7 km. The magnitude of tilt fluctuated by approximately 5 km on a 3–4-h time scale. In addition, the direction of tilt did not continuously rotate, but instead fluctuated from downshear left through downshear to downshear right. This suggests that a restoring mechanism was opposing the tendency of vertical shear to tilt the vortex and the tendency of the tilt vector to rotate.

Based on the results of this study and the simulations noted above, it is speculated that as long as a deep convective response to vertical shear is allowed, tropical cyclone tilt will be minimized in the inner core. In this view, the deep divergent circulation counteracts the influence of the shear in tilting the vortex and excites convection that diabatically modifies the PV structure of the inner core and maintains vertical alignment of the vortex (S. Jones 2002, personal communication). The small tilt makes it possible for upward motion and lightning to remain downshear and downshear left. The

presence of a deep convective response to shear was guaranteed in this study by the minimum flash criteria. The results do not necessarily extend to circumstances in which convection is suppressed. It is apparent that additional observations of the magnitude and direction of vortex tilt in the core of tropical cyclones in nature are needed to address the relationship between vertical shear and vortex tilt.

Figures 5a and 5b show a similar structure of the outer rainbands in the downshear right quadrant of both a hurricane over water and a tropical storm over land. This structure strongly resembles the stationary band complex of Willoughby et al. (1984) and the rain shield described by Senn and Hiser (1959). The only mechanism that places maximum upward motion in the downshear right quadrant is the adiabatic tilting mechanism (vortex flow on distorted vortex isentropes) described by Raymond (1992), Jones (1995), and Frank and Ritchie (1999). It was argued earlier that the storm core does not tilt. However, Jones (1995) showed that the region outside of the core has significantly greater tilt than that inside the radius of maximum winds in dry model simulations (her Fig. 6). The radii outside 100 km can have significant expanses of unsaturated air. It is thus possible that the dominant downshear right signature in outer bands relates to larger tilts in this region and to vertical motions organized primarily by dry adiabatic processes. No observations have been made of vortex tilt outside of the core in real tropical cyclones, and the dynamics of outer rainbands and their relationship to vertical wind shear remain prime topics for future observational and modeling studies.

Corbosiero (2000) showed that convective asymmetries were also influenced by storm motion, in a manner similar to that shown by previous studies. Further analysis showed that the motion influence was considerably weaker than the vertical shear influence. Nevertheless, both effects can exist simultaneously only if vertical wind shear and storm motion have a systematic relationship. The effects of storm motion on the lightning distribution, and the dynamics of the relationship between motion and shear, will be addressed in an upcoming paper.

Acknowledgments. We benefited greatly from discussions with Dr. Sarah Jones of the University of Munich and Dr. Robert Rogers of the Hurricane Research Division of NOAA. We are indebted to David Vollaro and Gretchen Heller for their help in developing computer programs to read and interpret the lightning data and the ECMWF gridded analyses. The latter were obtained from the National Center for Atmospheric Research, which is supported by the National Science Foundation. We thank Global Atmospherics, Inc., for providing processed lightning locations. This research was supported by National Science Foundation Grants ATM9423229 and ATM0000673 and Office of Naval Research Grant N00014-98-1-0599.

APPENDIX

Influence of Minimum Flash Count Criteria

The imposition of a minimum flash count criterion to the individual time periods in this study preferentially eliminated storms with certain characteristics. These characteristics will be investigated by examining distributions of vertical wind shear and average intensity for all 303 12-h periods, and for the 106 inner core and 154 outer rainband cases meeting their respective minimum flash criteria.

a. Vertical wind shear

Figure A1 shows the distribution of the vertical wind shear in the 303 individual cases examined. For shear of up to 13 m s^{-1}, the distribution resembles a rough double-peaked bell curve with a quick increase in the number of cases with very small shear (0–2 m s^{-1}) to a relative maximum in the distribution between 6–8 m s^{-1}, to a main peak between 11 and 12 m s^{-1}. The right side of the distribution, the high-shear values, exhibits a sharp decrease in the number of cases with shear greater than 13 m s^{-1}. This rapid decrease supports the notion that tropical cyclones cannot sustain themselves in environments where the vertical shear is greater than 12.5 m s^{-1} (Zehr 1992). The average magnitude of the shear in all cases is 9.3 m s^{-1}.

When the inner core flash criterion was applied to the periods, 38% of both the weak- and medium-shear time periods and 31% of the strong-shear time periods met the criterion. Thus, no vertical shear range was preferentially eliminated. The resulting number of 12-h periods in the inner core region for low, medium, and high shear were 23, 43, and 40, respectively.

In the outer rainband region, a much larger percentage of the weak- and medium-shear cases, 65% and 61% respectively, survived the flash criterion. Only 35% of the strong-shear time periods met the minimum flash

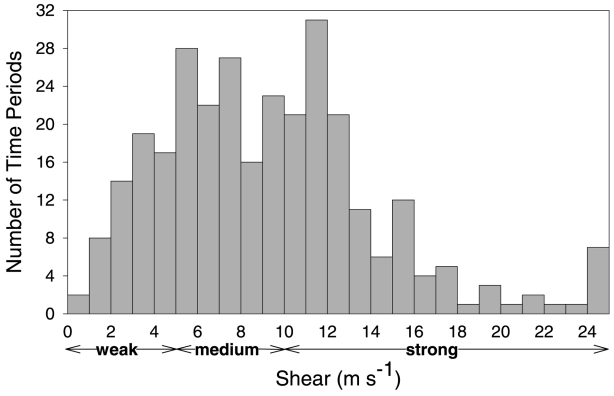

FIG. A1. Distribution of the magnitude of vertical wind shear (m s^{-1}) for all 303 12-h time periods. The three categories of shear (weak: <5 m s^{-1}; medium: 5–10 m s^{-1}; and strong: >10 m s^{-1}) used in the text are noted for reference.

count. Overall, 39 weak-, 70 medium-, and 45 strong-shear time periods were present in the outer band region. The reason for the relative lack of lightning in the outer rainbands in the presence of strong vertical shear is uncertain.

b. Storm intensity

Storm intensity, defined by the maximum surface wind speed, is available in the best track dataset every 6 h. Because we are dealing with 12-h time periods in this study an average intensity per 12-h period was calculated using a 1–2–1 weighting.

This study is restricted to the times when the storms were over land (145 time periods) or within 400 km of the coastline over water (158 time periods). The significant percentage of over-land time periods results in tropical depressions being most often represented (Fig. A2). Overall, 40% of the time periods studied here are tropical depressions, 34% tropical storms, and 26% hurricanes.

When just the time periods meeting the inner core flash criterion are considered, a significant change in the distribution of intensity occurs. For maximum wind speeds less than 33 m s^{-1} (the dividing line between tropical storms and hurricanes), the shape of the distribution looks much the same as when all time periods are examined, with 40% of the time periods meeting the criterion. For hurricane-strength time periods, however, only 16 of the original 79 (20%) meet the criterion, with 11 of those 16 being minimal (category 1) hurricanes with wind speeds less than 43 m s^{-1}. This distribution is consistent with the previous studies of Molinari et al. (1999) and Heller (1999), who found that the average ground flash density in the core was generally larger in tropical storms and marginal hurricanes than in strong hurricanes.

The outer rainband minimum flash criterion was met by 54% of the tropical depression and tropical storm time periods, and 43% of hurricane time periods. The latter are equally divided between marginal and strong hurricanes, and thus more strong hurricanes remain in the dataset for outer rainband regions than inner core regions.

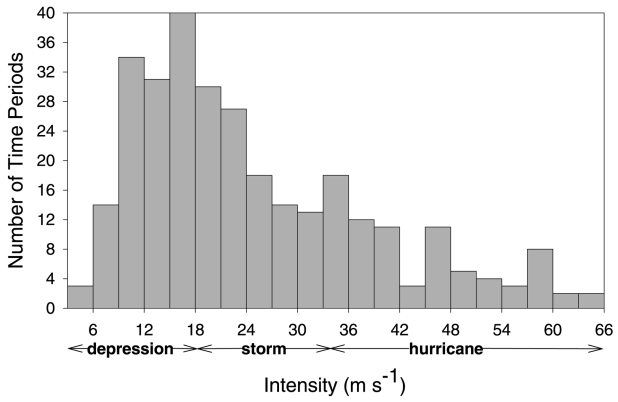

FIG. A2. Distribution of average intensity (defined by the maximum surface wind speed in m s^{-1}) for all 303 12-h time periods. The conventional classes of tropical cyclone strength are noted for reference.

REFERENCES

Bender, M. A., 1997: The effect of relative flow on the asymmetric structure of the interior of hurricanes. *J. Atmos. Sci.*, **54,** 703–724.

Black, M. L., R. W. Burpee, and F. D. Marks Jr., 1996: Vertical motion characteristics of tropical cyclones determined with airborne Doppler radial velocities. *J. Atmos. Sci.*, **53,** 802–822.

Bogner, P. B., G. M. Barnes, and J. L. Franklin, 2000: Conditional instability and shear for six hurricanes over the Atlantic Ocean. *Wea. Forecasting*, **15,** 192–207.

Cecil, D. J., and E. J. Zipser, 1999: Relationships between tropical cyclone intensity and satellite-based indicators of inner core convection: 85-GHz ice-scattering signature and lightning. *Mon. Wea. Rev.*, **127,** 103–123.

Corbosiero, K. L., 2000: The effects of vertical wind shear and storm motion on the distribution of lightning in tropical cyclones. M.S. thesis, Dept. of Earth and Atmospheric Sciences, University at Albany, State University of New York, 105 pp.

Cummins, K. L., W. L. Hiscox, A. E. Pifer, and M. W. Maier, 1992: Performance analysis of the U.S. National Lightning Detection Network. *Ninth Int. Conf. on Atmospheric Electricity*, St. Petersburg, Russia, Amer. Meteor. Soc., 914–919.

——, M. J. Murphy, E. A. Bardo, W. L. Hiscox, R. B. Pyle, and A. E. Pifer, 1998: A combined TOA/MDF technology upgrade of the U.S. National Lightning Detection Network. *J. Geophys. Res.*, **103,** 9035–9044.

DeMaria, M., 1996: The effect of vertical shear on tropical cyclone intensity change. *J. Atmos. Sci.*, **53,** 2076–2087.

——, and J. Kaplan, 1994: A statistical hurricane intensity prediction scheme (SHIPS) for the Atlantic Basin. *Wea. Forecasting*, **9,** 209–220.

Frank, W. M., and E. A. Ritchie, 1999: Effects of environmental flow upon tropical cyclone structure. *Mon. Wea. Rev.*, **127,** 2044–2061.

——, and ——, 2001: Effects of vertical wind shear on hurricane intensity and structure. *Mon. Wea. Rev.*, **129,** 2249–2269.

Franklin, J. L., S. J. Ford, S. E. Feuer, and F. D. Marks Jr., 1993: The kinematic structure of Hurricane Gloria (1985) determined from nested analyses of dropwindsonde and Doppler radar data. *Mon. Wea. Rev.*, **121,** 2433–2451.

Gamache, J. F., H. E. Willoughby, M. L. Black, and C. E. Samsury, 1997: Wind shear, sea surface temperature and convection in hurricanes observed by airborne Doppler radar. *22nd Conf. on Hurricanes and Tropical Meteorology*. Fort Collins, CO, Amer. Meteor. Soc., 121–122.

Gray, W. M., 1968: Global view of the origin of tropical disturbances and storms. *Mon. Wea. Rev.*, **96,** 669–700.

Hanley, D. E., J. Molinari, and D. Keyser, 2001: A composite study of the interactions between tropical cyclones and upper tropospheric troughs. *Mon. Wea. Rev.*, **129,** 2570–2584.

Heller, G., 1999: Lightning variations in landfalling tropical cyclones. M.S. thesis, Dept. of Earth and Atmospheric Sciences, State University of New York at Albany, 138 pp.

Idone, V. P., D. A. Davis, P. K. Moore, Y. Wang, R. W. Henderson, M. Ries, and P. F. Jamason, 1998a: Performance evaluation of the National Lightning Detection Network in eastern New York. Part I: Detection efficiency. *J. Geophys. Res.*, **103,** 9045–9055.

——, ——, ——, ——, ——, ——, and ——, 1998b: Performance evaluation of the National Lightning Detection Network in eastern New York. Part II: Location accuracy. *J. Geophys. Res.*, **103,** 9057–9069.

Jones, S. C., 1995: The evolution of vortices in vertical shear: I:

Initially barotropic vortices. *Quart. J. Roy. Meteor. Soc.,* **121,** 821–851.
——, 2000: The evolution of vortices in vertical shear: III: Baroclinic vortices. *Quart. J. Roy. Meteor. Soc.,* **126,** 3161–3185.
Krider, E. P., R. C. Noggle, and M. A. Uman, 1976: A gated, wideband magnetic direction finder for lightning return strokes. *J. Applied Meteor.,* **15,** 301–306.
Lyons, W. A., and C. S. Keen, 1994: Observations of lightning in convective supercells within tropical storms and hurricanes. *Mon. Wea. Rev.,* **122,** 1897–1916.
Molinari, J., and D. Vollaro, 1989: External influences on hurricane intensity. Part I: Outflow layer eddy momentum fluxes. *J. Atmos. Sci.,* **46,** 1093–1105.
——, and ——, 1990: External influences on hurricane intensity. Part II: Vertical structure and response of the hurricane vortex. *J. Atmos. Sci.,* **47,** 1902–1918.
——, ——, and F. Robasky, 1992: Use of ECMWF operational analyses for studies of the tropical cyclone environment. *Meteor. Atmos. Phys.,* **47,** 127–144.
——, P. K. Moore, V. P. Idone, R. W. Henderson, and A. B. Saljoughy, 1994: Cloud-to-ground lightning in Hurricane Andrew. *J. Geophys. Res.,* **99,** 16 665–16 676.
——, S. Skubis, and D. Vollaro, 1995: External influences on hurricane intensity. Part III: Potential vorticity evolution. *J. Atmos. Sci.,* **52,** 3593–3606.
——, P. Moore, and V. Idone, 1999: Convective structure of hurricanes as revealed by lightning locations. *Mon. Wea. Rev.,* **127,** 520–534.
Orville, R. E., 1991: Calibration of a magnetic direction finding network using measured triggered lighting return stroke peak currents. *J. Geophys. Res.,* **96,** 17 135–17 142.
——, 1994: Cloud-to-ground lightning flash characteristics in the contiguous United States: 1989–1991. *J. Geophys. Res.,* **99,** 10 833–10 841.
——, R. A. Weisman, R. B. Pyle, R. W. Henderson, and R. E. Orville Jr., 1987: Cloud-to-ground lighting flash characteristics from June 1984 through May 1985. *J. Geophys. Res.,* **92,** 5640–5644.
Raymond, D. J., 1992: Nonlinear balance and potential vorticity thinking at large Rossby number. *Quart. J. Roy. Meteor. Soc.,* **118,** 987–1015.
Reasor, P. D., M. T. Montgomery, F. D. Marks Jr., and J. F. Gamache, 2000: Low-wavenumber structure and evolution of the hurricane inner core observed by airborne dual-Doppler radar. *Mon. Wea. Rev.,* **128,** 1653–1680.
Samsury, C. E., and R. E. Orville, 1994: Cloud-to-ground lightning in tropical cyclones: A study of Hurricanes Hugo (1989) and Jerry (1989). *Mon. Wea. Rev.,* **122,** 1887–1896.
Senn, H. V., and H. W. Hiser, 1959: On the origin of hurricane spiral bands. *J. Meteor.,* **16,** 419–426.
Wang, Y., and G. J. Holland, 1996: Tropical cyclone motion and evolution in vertical shear. *J. Atmos. Sci.,* **53,** 3313–3332.
Willoughby, H. E., F. D. Marks Jr., and R. J. Feinberg, 1984: Stationary and moving convective bands in hurricanes. *J. Atmos. Sci.,* **41,** 3189–3211.
Zehr, R. M., 1992: Tropical cyclogenesis in the Western Pacific. NOAA Tech. Rep. NESDIS 61, 181 pp.